Glucose-6-phosphate dehydrogenase and MEG3 controls hypoxia-induced expression of serum response factor (SRF) and SRF-dependent genes in pulmonary smooth muscle cell

Atsushi KITAGAWA, Christina JACOB and Sachin A. GUPTE

Department of Pharmacology, New York Medical College, BSB 546, 15 Dana Road, Valhalla,
*NY 10595, USA*

Abstract

Although hypoxia induces aberrant gene expression and dedifferentiation of smooth muscle cells (SMCs), mechanisms that alter dedifferentiation gene expression by hypoxia remain unclear. Therefore, we aimed to gain insight into the hypoxia-controlled gene expression in SMCs. We conducted studies using SMCs cultured in 3% oxygen (hypoxia) and the lungs of mice exposed to 10% oxygen (hypoxia). Our results suggest hypoxia upregulated expression of transcription factor CP2-like protein1, krüppel-like factor 4, and E2f transcription factor 1 enriched genes including basonuclin 2 (*Bcn2*), serum response factor (*Srf*), polycomb 3 (*Cbx8*), homeobox D9 (*Hoxd9*), lysine demethylase 1A (*Kdm1a*), etc. Additionally, we found that silencing glucose-6-phosphate dehydrogenase (G6PD) expression and inhibiting G6PD activity downregulated *Srf* transcript and hypomethylation of SMC genes (*Myocd*, *Myh11*, and *Cnn1*) and concomitantly increased their expression in the lungs of hypoxic mice. Furthermore, G6PD inhibition hypomethylated MEG3, a long noncoding RNA, gene and upregulated MEG3 expression in the lungs of hypoxic mice and in hypoxic SMCs. Silencing MEG3 expression in SMC mitigated the hypoxia-induced transcription of *SRF*. These findings collectively demonstrate that MEG3 and G6PD codependently regulate *Srf* expression in hypoxic SMCs. Moreover, G6PD inhibition upregulated SRF-MYOCD-driven gene expression, determinant of a differentiated SMC phenotype.

Key words: hypoxia, smooth muscle cells, glucose-6-phosphate dehydrogenase (G6PD), MEG3, pulmonary hypertension

Corresponding author: Sachin A. Gupte, MD, PhD, Department of Pharmacology, New York Medical College, BSB 546, 15 Dana Road, Valhalla, NY 10595, USA
E-mail: sachin_gupte@yahoo.com

Highlights

- G6PD contributes to the upregulation of *Srf* and the downregulation of SMC genes (*Myocd*, *Cnn1*, and *Myh11*)
- G6PD-mediated DNA methylation suppressed the expression of SRF-MYOCD-driven genes
- MEG3 knockdown increased hypoxia-induced *Srf* expression
- G6PD inhibition enhanced MEG3 expression and suppressed *Srf* expression in a MEG-dependent manner
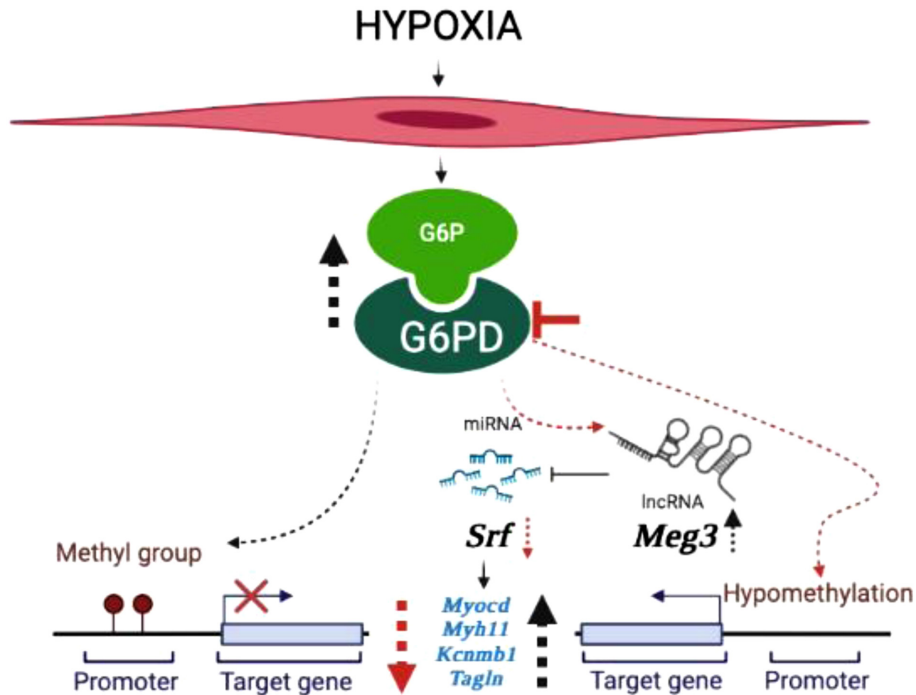
Graphical Abstract

Introduction

Hypoxic stimulus alters metabolism and gene expression in the cell. These adaptive metabolic and transcriptomic reprogramming are primarily mediated by the activation of hypoxia-inducible factors. Parallelly, hypoxia elicits reactive oxygen species generation and redox changes in smooth muscle cells (SMCs) (1). Increased reactive oxygen species and redox changes modify gene expression program (2), however the redox-dependent mechanism(s) that mediates hypoxia-induced genetic reprogramming that contribute to the fate and plasticity of SMC remains unclear.

SMCs exhibit plasticity within blood vessels, and the SMC phenotype is modulated by turbulent blood flow, biochemical changes, and environmental stimuli such as hypoxia. SMCs may exist in a differentiated (physiological/contractile) or dedifferentiated (hyperproliferative and synthetic) state; a heterogeneous population (different phenotypic states) of SMCs is found in the medial layer of pulmonary arteries (PAs) (3, 4). SMCs convert from a differentiated to a dedifferentiated phenotype under several conditions, including chronic hypoxia (5–7). However, our knowledge of hypoxia-regulated gene expression and SMC plasticity remains incomplete. SMC plasticity is controlled by transcription factors serum response factor (*Srf*) and co-activator

myocardin (MYOCD) and krüppel-like factors 4 and 5 (KLF4 and KLF5) (7). SRF-MYOCD promotes expression of SMC-restricted genes and maintains SMCs in a differentiated state, while KLFs promote downregulation of SMC-restricted genes and switching from a differentiated to a dedifferentiated phenotype. Decreased MYOCD and increased KLFs tip the balance toward the synthetic or dedifferentiated SMC phenotype (1, 8–10).

The ability of the SMCs in the medial layer of PAs to contract and relax in a pulsatile manner is central to the high compliance and low resistance of the pulmonary circulation. The maladaptation of SMCs to environmental stress-stimuli within PAs leads to remodeling of arteries and increases in pulmonary vascular resistance. Hyperproliferative and apoptosis-resistant vascular cells contribute to abnormal vascular remodeling (11, 12). SMCs undergo metabolic reprogramming to support the high rate of proliferation they exhibit. Both aerobic glycolysis and glucose flux through the pentose phosphate pathway (PPP), a branch of glycolysis that is vital to cell growth and survival, are increased in various cell types within the pulmonary arterial wall in hypertensive patients and animal models (1, 13–17). However, the mechanism through which the increased PPP activity, observed in hypoxic condition (1), promotes expression of genes responsible for increasing maladaptive SMCs that contribute to pulmonary remodeling remains unclear.

One of the major functions of long non-coding RNAs (lncRNAs), as biologically active molecules, is to regulate the expression of adjacent protein-coding genes. LncRNAs are epigenetic modifiers that regulate gene expression at transcriptional and post-transcriptional levels (18). Dysregulation of lncRNAs is associated with the pathogenesis of diseases such as cancers, immune-related diseases, respiratory diseases, and cardiovascular diseases (19–21). To-date, many lncRNAs have been identified, and more are being identified, and characterized in endothelial cells and SMCs (21–24). Lately, the role of some lncRNAs in the regulation of gene expression and SMC phenotype has been recognized (21–23, 25). Notably, MEG3, a lncRNA, has been linked to endothelial cell senescence and SMC proliferation (21, 24). MEG3 facilitate lysine demethylase (JARID2) and polycomb repressive complex 2 (PRC2) interaction on chromatin resulting in increased H3K27me3, a heterochromatin mark (26). JARID activity is regulated by the metabolites of the glycolytic pathway and Krebs cycle. The PPP intermediates modulate the activity of the glycolytic pathway and Krebs cycle (27, 28). Furthermore, inhibition or knockdown of glucose-6-phosphate dehydrogenase (G6PD), the rate-limiting enzyme of PPP and source of cellular redox potential, reduces SMC proliferation (1, 29). G6PD expression and activity is rapidly (within 30 min) increased in SMCs by hypoxia-induced reactive oxygen species (1). Elevated G6PD expression and/or activity augments reductive stress (30), which contributes to SMC proliferation (31) Since, G6PD and MEG3 has been implicated in regulating SMC proliferation, we speculated that G6PD and MEG3 independently or dependently regulate *Srf* and SRF-dependent gene program and could be critical in mediating hypoxia-induced changes in expression of genes in SMCs and phenotype of SMCs. Therefore, our goal was to determine whether there is any interdependency between the PPP/G6PD and MEG3 signaling controls expression of genes involved in regulating SMC plasticity. Here, we determine whether G6PD inhibition resets the SMC-restricted genes by upregulating MEG3 in the lungs of hypoxic mice and in the SMCs exposed to hypoxia. Our findings reveal novel cross-talk between G6PD and MEG3 signaling is pivotal to the regulation of hypoxia-induced expression of SMC dedifferentiation genes.

Materials and Methods

Data availability

The authors confirm that the data supporting the findings of this study are available within the article [and/or] its supplementary materials.

Drugs and reagents

All chemicals were purchased from Sigma, Thermo Fisher, or VWR. Human pulmonary artery smooth muscle cells (SMCs) were purchase from Lonza (MD, USA).

Animal models and experimental protocols

All animal experiments were approved (No. 30-1-0517) by the New York Medical College Animal Care and Use Committee. Male and female C57BL/6 J mice (18–32 g) were purchased from the Jackson Laboratory and randomly divided into normoxia (Nx) and hypoxia (Hx) groups. Mice in the Nx group were placed in a normoxic (21% O_2) environment. The Hx group was placed in a normobaric hypoxic chamber (10% O_2) for 6 weeks. In a separated group, mice received daily subcutaneous injections of a novel G6PD inhibitor, N-[(3β,5α)-17-oxoandrostan-3-yl]sulfamide (4091; 1.5 mg kg^{-1} day^{-1}) (32), for last 3 weeks of hypoxia. We have recently found that 4091 treatment inhibits G6PD activity in lungs of mice exposed to hypoxia (33). Mice were also intratracheally administered aerosolized AdGFP-G6PD-shRNA (IT-shG6PD), which reduces expression of G6PD, or AdGFP-scrambled-shRNA (given once a week) during weeks 3 and 4 (27). At the end of the treatment, mice were anesthetized with isoflurane (induced at 3% and maintained at 1.5%) and which tissue (lungs and arteries) and blood samples were collected.

Cell culture

Human SMCs were maintained at 37 °C under 5% CO_2 in SmBM™ smooth muscle basal medium (Lonza, #CC-3181) supplemented with a SmGM™-2 SingleQuots kit (Lonza, #CC-4149). Once cells reached approximately 70% confluence, they were sub-cultured using 0.05% trypsin-EDTA (GIBCO, Cat #25300-054, Thermo Fischer Scientific, Grand Island, NY, USA) into 6-well plates at about 3×10^5 cells/well density. Cells were cultured in 21% O_2 (normoxia) or in 3% O_2 (hypoxia).

Immunofluorescent staining

We performed immunofluorescent staining as described previously (1). Briefly, lung sections (5 µm) were deparaffinized and heated with 1× citrate buffer. Endogenous peroxidase activity was suppressed with 3% H2O2 treatment. Sections were blocked with blocking serum (Vectastain Universal Elite ABC kit; Vector Laboratories, Burlingame, CA, USA). Slides were incubated with primary antibodies over night at 4 °C. Sections were incubated with Alexa Fluor-conjugated secondary antibodies (Life Technologies) for 1 h at room temperature. The nucleus was stained with DAPI (1 µg/ml). Imaging was done via Axio imager M1 microscope, Axiocam MRm camera, and AxioVision microscopy software (Carl Zeiss, Jena, Germany).

MEG3 siRNA transfection

Cells were transfected with MEG3 siRNA (50 nM) or Scrambled Control (50 nM). After transfection for 48 h, the cells were washed three times using PBS and harvested in Qiazol (700 µl). The extracted RNA was later used for quantitative real time PCR (RT-PCR).

Quantitative real time PCR

Real time RT-PCR was used to analyze mRNA expression. Briefly, total RNA was extracted from lungs using a Qiagen kit (Cat #217004). The input RNA quality and concentration were measured with a Synergy HT Take3 Microplate Reader (BioTek, Winooski, VT, USA), and cDNA was prepared using SuperScript IV VILO Master Mix (Cat #11756500, Invitrogen). RT-PCR was performed in duplicate using TaqMan™ Fast Advanced

Master Mix (Cat #44-445-57, ThermoFischer) for mRNA using an Mx3000P RT-PCR System (Stratagene, Santa Clara, CA, USA). The primers for the PCR were purchased from Thermo Fisher Scientific (TaqMan). Results were normalized using an internal control (*Tuba1a*).

RNA-Seq analysis

After collecting lung tissue samples from normotensive and PH mice, total RNA was isolated from lungs using an AllPrep DNA/RNA/miRNA Universal Kit (Qiagen) according to the manufacturer's instructions. RNA was quantified using NanoDrop™ (ThermoFisher), and quality was assessed using an Agilent 2100 Bioanalyzer. RNA-seq library were constructed using a TruSeq Stranded Total RNA Preparation kit (Illumina) with 200 ng of RNA as input according to the manufacturer's instructions. Libraries were sequenced on a HiSeq 2500 System (Illumina) with single-end reads of 100 nt at the University of Rochester Genomics Research Center. Single-end sequencing was done at a depth of 10 million reads per replicate (n=3). Quantitative analysis, including statistical analysis of differentially expressed genes, was conducted with Cufflinks 2.0.2 and Cuffdiff2 (http://cufflinks.cbcb.umd.edu). The Benjamini-Hochberg method was applied for multiple test correction (FDR < 0.05).

Reduced Representation Bisulfite Sequencing (RRBS)

Genomic DNA was isolated from lung tissue samples using AllPrep DNA/RNA/miRNA Universal Kit (Qiagen) according to the manufacturer's instructions. DNA was quantified using NanoDrop™ (ThermoFisher) and Qubit Fluorometer (ThermoFisher). Genomic DNA quality was assessed using an Agilent TapeStation. RRBS libraries were constructed using a Premium RRBS Kit (Diagenode) following the manufacturer's instructions. Libraries were sequenced on a HiSeq 2500 System (Illumina) with paired-end reads of 125 nt. Raw reads generated from the HiSeq 2500 sequencer were demultiplexed using bcl2fastq (version 2.19.0). Quality filtering and adapter removal were performed using Trim Galore (version 0.4.4_dev) with the following parameters: "–paired–clip_R1 3–clip_R2 3–three_prime_clip_R1 2–three_prime_clip_R2 2" (http://www.bioinformatics.babraham.ac.uk/projects/ trim_galore/). Processed and cleaned reads were then mapped to the mouse reference genome (mg38) using Bismark (version 0.19.0) with the following parameters: "–bowtie2–maxins 1000". Differential methylation analysis was performed using methylKit (version 1.4.0) within an R (version 3.4.1) environment. Bismark alignments were processed using methylKit in the CpG context with a minimum quality threshold of 10. Coverage was normalized after filtering for loci with a coverage of at least five reads and no more than the 99.9th percentile of coverage values. The coverage was then normalized across samples, and the methylation counts were aggregated for 500 nt windows spanning the entire genome. A unified window set across samples was derived such that only windows with coverage by at least one sample per group were retained. Differential methylation analysis between conditional groups was performed using the χ^2 test, applying a q-value (SLIM) threshold of 0.05 and a methylation difference threshold of 25%.

Statistical analysis

Statistical analysis was performed using GraphPad Prism 9 software. Values are presented as means ± standard error (SE). Multiple comparisons were made using one-way ANOVA followed by Sidak's post-hoc test. Values of $P<0.05$ were considered significant.

Results

G6PD regulates gene expression in the lungs of hypoxic mice

To compare the gene expression profiles in the lungs of mice exposed to Nx, Hx, or Hx+4091, we performed RNA-seq analysis and found that 352 genes were upregulated and 4310 were downregulated in the lungs of Hx-mice as compared to those in the lungs of Nx-mice, whereas 21 were upregulated and 2119 were downregulated in the lungs of Hx+4091 mice as compared to those in the lungs of Hx-mice. Among the top upregulated (>2-fold) genes in the lungs of Hx-mice vs. Nx-mice (Fig. 1A), the first two, basonuclin-2 (*Bnc2*) and *Srf*, encode transcription factors, and the third gene on the list, chromobox8 (*Cbx8*), encodes a protein that is a component of the polycomb group multiprotein (PRC1)-like complex, which maintains the transcriptionally repressed state of many genes. G6PD inhibition suppressed pulmonary expression of the top 15 upregulated genes (Fig. 1A) and normalized their expression level to the baseline of the top 13 downregulated genes (>2-fold) in the lungs of Hx-mice (Fig. 1A).

We next performed transcription factor binding site (TFBS) enrichment analysis using oPOSSUM (34). This analysis revealed that TFCP2l1, KLF4, and E2F1 were the most enriched transcription factors on genes upregulated by Hx vs. Nx, and REST, HOXA5, PDX1, and PRRX2 were most enriched on genes downregu-
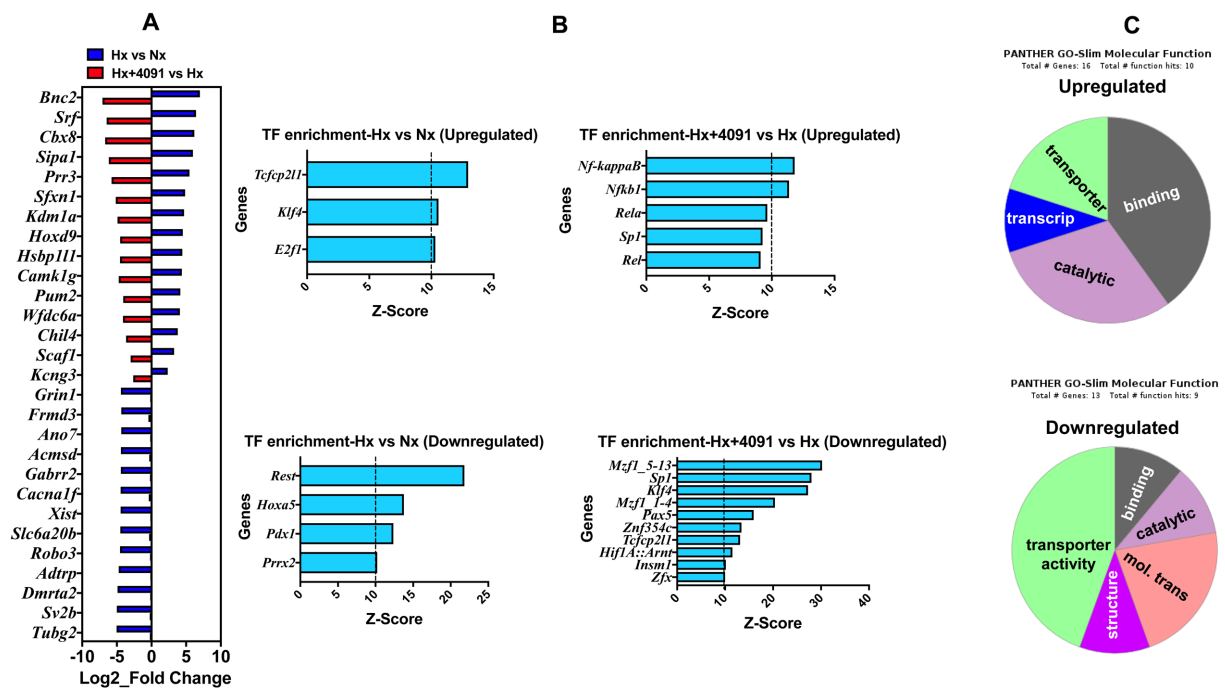

Fig. 1. G6PD inhibition modulates the gene expression program in the lungs of Hx-mice. A) RNA-seq results demonstrate *Bnc2* and *Srf* genes are the most upregulated in the lungs of Hx-mice (vs. Nx-mice). 4091 (1.5 mg kg^{-1} day^{-1}) administration to Hx-mice (Hx+4091) decreased their expression level. Downregulated genes in the lungs of Hx-mice were not affected by 4091. N=3 in each group. Statistical analysis was performed using the FDR test (adjusted *P<0.05*). B) TFBS enrichment analysis using oPOSSUM revealed that in TCFCP2L1 and KLF4 were the most enriched on upregulated genes, and REST and HOXA5 TFBSs were the most enriched on downregulated genes in the lungs of Hx-mice. Administration of 4091 to Hx-mice upregulated genes enriched with NFκB and RELA but downregulated genes enriched with MZF1, SP1, and KLF4. C) PANTHER GO term analysis revealed binding, catalytic, transcription, and transporter activities were affected by upregulated genes in the lungs of Hx-mice vs Nx-mice, whereas binding, catalytic, molecular transducer, structural, and transporter activities were affected by downregulated genes in the lungs of Hx-mice vs. Nx-mice.

lated by Hx vs. Nx (Fig. 1B). In contrast, NFκB, RELA, and SP1 were most enriched on genes upregulated by Hx+4091 vs. Hx (Fig. 1B, top panels), and MZF1, SP1, KLF4, PAX5, and HIF1A::ARNT TFBSs were most enriched on genes downregulated by Hx+4091 vs. Hx (Fig. 1B, bottom panels).

GO term analysis between Hx-mice and Nx-mice revealed that the upregulated genes supported molecular functions such as binding, catalytic activity, transporter activity, and transcription (Fig. 1C, top panel), while the downregulated genes supported molecular transducer activity and structural molecule activity, in addition to supporting binding, catalytic activity, and transporter activity (Fig. 1C, bottom panel).

Real time PCR analysis of the expression of pumilio RNA binding family member 2 (*Pum2*; Fig. 2A), which encodes an RNA-binding protein that functions as a translational repressor during cell differentiation and a positive regulator of cell proliferation in adipose-derived stem cells, and Doublesex- And Mab-3-Related Transcription Factor A2 (*Dmrta2*; Fig. 2B), which shows DNA-binding transcription factor activity and sequence-specific DNA binding, confirmed the RNA-seq results. We randomly selected these genes for RT-PCR based on their function in the transcription processes.

G6PD inhibition decreases pulmonary Srf expression and increases expression level of SRF-MYOCD-dependent genes in Hx-mice

SRF and the transcription co-activator MYOCD are specifically expressed in SMCs (35–37). SRF-MYOCD is important for maintaining expression of SMC-restricted genes such as myosin heavy chain 11 (*Myh11*) and calponin1 (*Cnn1*) and keeps the cells in a differentiated state. However, SRF can also interact with other transcription co-regulators, when MYOCD is low, to promote SMC dedifferentiation and proliferation (38). Because pulmonary *Srf* expression is elevated in hypoxic mice, we speculated that the pulmonary expression levels of the SRF-MYOCD-driven genes *Myh11* and *Cnn1* would be increased in hypoxic mice. In RNAseq analysis, we found expression of *Myocd* and SRF-MYOCD-dependent genes was decreased in lungs Hx vs Nx mice, however the decrease was less than 1-fold and treatment of 4091 to Hx mice increased their expression. To confirm these RNA-seq findings, we used RT-PCR to measure expression of *Srf, Myocd, Cnn1*, and *Myh11* in the lungs of mice treated with 1] Nx, 2] Hx, 3] Hx+4091, or 4] Hx+G6PD-shRNA. As expected *Srf* expression level was elevated in the lungs of hypoxic mice as compared to that in the lungs of their corresponding Nx controls. Additionally, G6PD inhibition with 4091 decreased pulmonary *Srf* expression in
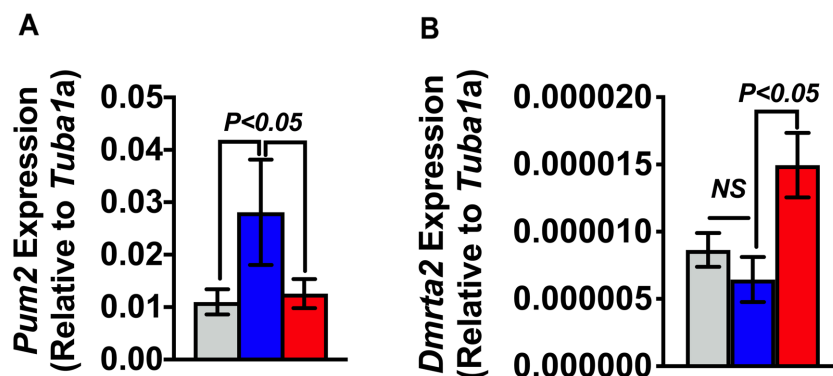

Fig. 2. G6PD inhibition decreases *Pum2* and increases *Dmtra2* expression in the lungs of Hx-mice. To confirm RNAseq results, we performed RT-PCR of one up- and down-regulated gene. RT-PCR confirmed that 4091 (1.5 mg kg^{-1} day^{-1}) downregulated *Pum2* expression (A) and upregulated *Dmrta2* expression (B) in the lungs of Hx-mice. Gray bar=Control; Blue bar=Hx; and Red bar=Hx+4091. N=5 (males=3 and females=2) in each group. Statistical analysis was performed using one-way ANOVA and Sidak's test for multiple comparisons.

these mice (Fig. 3A). Conversely, pulmonary expression levels of *Myocd* (Fig. 3B), *Cnn1* (Fig. 3C and E), and *Myh11* (Fig. 3F) were lower in hypoxic mice than in normoxic mice, but their expression levels were restored in mice treated with Hx+4091 (Fig. 3B–D). At the same time, pulmonary expression levels of *Cnn1* (Fig. 3E) and *Myh11* (Fig. 3F) were higher in the Hx+G6PD-shRNA group than in the Hx group. Similarly, expression of CNN1 and MYH11 increased in pulmonary arteries by 4091 and G6PD-shRNA treatment (Fig. 3G).

G6PD inhibition prevents hypoxia-induced DNA methylation of Myocd and SRF-MYOCD-driven genes

How is *Myocd* and SRF-MYOCD-driven gene expression regulated? Based on recent studies (27, 39), we speculated that G6PD inhibition would decrease DNA methylation in mice, thereby normalizing gene expression. In the lungs of Hx-mice, 4091 treatments led to hypomethylation of *Myocd*, *Myh11*, *Mylk*, *Myl9*, *Kcnmb1*, and *Csrp2* (markers of differentiated SMCs driven by SRF-MYOCD; Table 1). All genes associated with the SMC contractile phenotype program, including *Myocd*, *Myh11*, *Cnn1*, *Lmod1* and *Kcnmb1*, as well as *Meg3*, which encodes a lncRNA that inhibits SMC proliferation (21), were hypomethylated in different CpG regions including; promoter, enhancer and transcription factor binding sites (Table 1). The critical SMC genes, such as *Myocd* and *Myh11*, and others were hypermethylated in the lungs of Hx-mice (Table 1). At the same time, expression of *Kcnmb1*, which encodes β-subunit of big-conductance Ca^{2+}-activated K^+ channels (BK_{ca}),
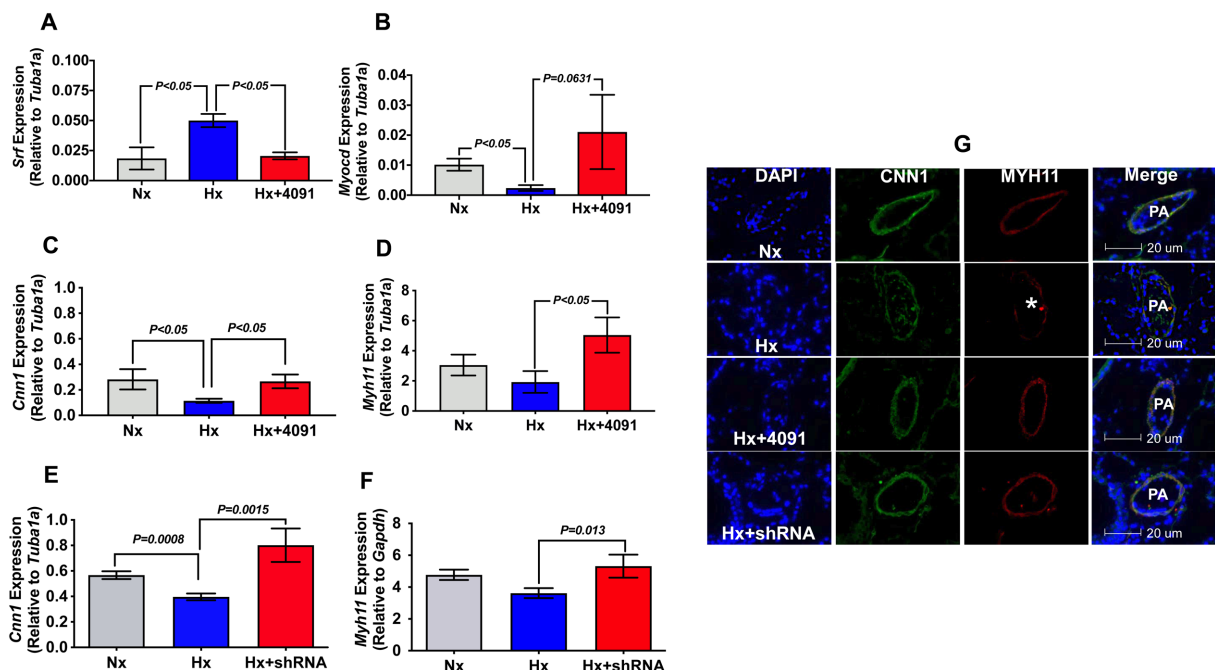

Fig. 3. SMC genes are upregulated in the lungs of Hx+4091-mice compared to those in the lungs of Hx-mice. Real time PCR demonstrating that pulmonary *Srf* (A) and *Myocd* (B) expression level is respectively decreased and increased by 4091 (1.5 mg kg^{-1} day^{-1}) in Hx. Increased pulmonary expression level of *Cnn1* (C) and *Myh11* (D) by 4091 in Hx-mice. E, F) Nasal administration of adenovirus carrying G6PD-shRNA (10^{-12} Pfu), as described previously (27), for 2 weeks increases pulmonary expression levels of *Cnn1* and *Myh11* in Hx-mice. G) Representative immunofluorescence micrographs of five different experiments showing that CNN1 and MYH11 are reduced in PAs in the lungs of Hx-mice as compared with those in the lungs of Nx-mice. Administration of 4091 and shRNA to Hx-mice prevented decrease of CNN1 and MYH11. N=5 (male=3 and female=2) in each group. Statistical analysis was performed using the one-way ANOVA (A to F). Sidak's test was used to compare multiple groups after ANOVA analysis.

Table 1. RRBS analysis showing differentially methylated CpG regions in *Myocd* and SRF-MYOCD-driven genes in the lungs of Hx- vs. Nx-mice and Hx+4091- vs. Hx-mice

Genes	Hx+4091 vs. Hx				Hx vs. Nx			
	% DM	Dist. to TSS	Strand	q-value	% DM	Dist. to TSS	Strand	q-value
ENSMUST00000121731.7_Actg2	39.4	3,991	−	0.009	−26.9	−10,237	−	6.60E-07
ENSMUST00000027677.7_Csrp1	−33.3	5,856	+	1.20E-05	31.9	5,856	+	3.30E-05
ENSMUST00000020403.5_Csrp2	−38.3	11,326	+	5.90E-08	38.2	11,326	+	1.40E-09
ENSMUST00000020403.5_Csrp2	−35.6	11,826	+	0.002	35.6	11,826	+	6.40E-05
ENSMUST00000035661.5_Cspg4	−85.1	−3,104	+	1.60E-14	77.1	−3,104	+	3.70E-10
ENSMUST00000035661.5_Cspg4	−33.3	15,899	+	0.0007	NDM			
ENSMUST00000020362.2_Kcnmb1	−35.8	−513	+	9.90E-09	45.1	−513	+	6.10E-11
ENSMUST00000020362.2_Kcnmb1	−40.0	−17,013	+	6.70E-07	NDM		+	
ENSMUST00000020362.2_Kcnmb1	−76.3	490	+	9.60E-08	29.3	490	+	0.003
ENSMUST00000020362.2_Kcnmb1	−27.9	9,490	+	5.20E-06	NDM			
ENSMUST00000203607.1_Klf15	52.3	0	+	8.50E-33	NDM			
ENSMUST00000059352.2_Lmod1	−31.5	696	+	0.003	−28.1	696	+	0.0004
ENSMUST00000146701.7_Meg3	−28.1	105	+	5.00E-11	NDM			
ENSMUST00000090287.3_Myh11	−92.9	48,409	−	5.20E-08	92.9	48,409	−	4.50E-08
ENSMUST00000088552.6_Myl9	−33.3	−4,920	+	1.20E-11	NDM			
ENSMUST00000023538.8_Mylk	−38.6	−10,921	+	1.70E-06	NDM			
ENSMUST00000023538.8_Mylk	−40.3	−11,921	+	0.003	NDM			
ENSMUST00000023538.8_Mylk	−29.4	−36,421	+	3.30E-07	NDM			
ENSMUST00000023538.8_Mylk	−37.5	52,582	+	0.002	NDM			
ENSMUST00000023538.8_Mylk	−25.2	73,582	+	0.001	NDM			
ENSMUST00000021922.9_Msx2	32.5	−3,428	−	2.00E-06	NDM			
ENSMUST00000101042.8_Myocd	−100.0	9,060	−	9.80E-07	39.0	9,060	−	0.02
ENSMUST00000034590.2_Tagln	−44.4	2,559	−	0.0002	26.3	2,559	−	0.007

DM: differential methylation of CpG region; NDM: no differential methylation; Dist to TSS: distance to transcription start site.

Table 2. RNA-seq analysis showing expression of BKca channel genes in the lungs of Hx- or Hx+4091-mice

Genes	Hx vs. Ctrl		Hx+4091 vs. Hx	
	Log2_fold	P-value	Log2_fold	P-value
Kcnma1	−2.0	0.0425	0.3	0.6801
Kcnmb1	−2.1	0.0242	0.1	0.8770
Kcnmb2	−1.3	0.0672	0.6	0.3623

and genes encoding other BK_{ca} channel subunits was suppressed in Hx-mice (Table 2). G6PD inhibition normalized *Kcnmb1* expression, but led to hypermethylation of *Klf15*, *Msx2,* and *Actg2* that are associated with dedifferentiated SMC phenotype. This suggests G6PD inhibition modifies DNA methylation status across the genome, including SMC genes, but not *Srf*, in the lungs of Hx-mice.

Inhibition and knockdown of G6PD increases MEG3 levels in the lungs of hypoxic mice

Recent studies suggest that downregulation of MEG3 expression in the lungs and PAs of idiopathic PH patients promotes hyperproliferation of SMCs (21). Therefore, we measured pulmonary MEG3 expression in mice exposed to: 1] Nx, 2] Hx, 3] Hx+4091, or 4] Hx+G6PD-siRNA. Although pulmonary MEG3 expression did not change in hypoxic mice as compared with that in normoxic mice (Fig. 4A), G6PD inhibition or knockdown increased pulmonary MEG3 expression level in hypoxic mice (Fig. 4A and B).
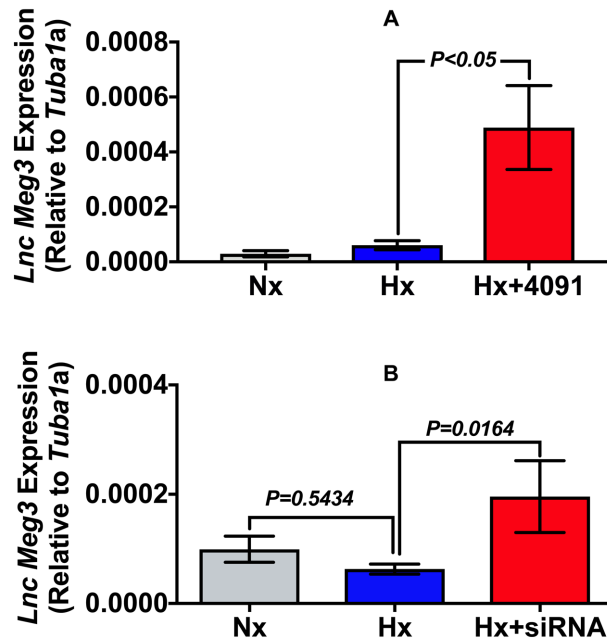
Fig. 4. Meg3 expression is upregulated by G6PD inhibition or knockdown in Hx lungs. A) Adminis-
tration of 4091 (1.5 mg kg^{-1} day^{-1}; N=5; male=3 and female=2) or B) shRNA (10^{-12} Pfu; N=6;
male=3 and female=3) increased pulmonary expression level of Meg3 in Hx-mice. N=5 in each
group. Statistical analysis was performed using one-way ANOVA. Sidak's test was used to com-
pare multiple groups after ANOVA analysis.

Inhibition of G6PD activity increases MEG3 level in SMC

Next, to determine whether there is any interdependency between the PPP-G6PD and MEG3 signaling,
we determined whether inhibiting G6PD activity regulates MEG3 expression in human SMCs cultured under
Nx and Hx. MEG3 expression decreased in Nx-SMCs (by 75%) and Hx-SMCs (by 50%) by knocking down
MEG3 (Fig. 5A). MEG3 levels in Hx-SMCs increased upon G6PD inhibition as compared Nx-SMCs, and this
increase was blocked by knocking down MEG3 by 68% in Nx-SMCs and 78% in Hx-SMCs (Fig. 5A).

G6PD inhibition and MEG3 decreases Srf expression in SMCs

Next, to determine whether increase in MEG3 level, induced by G6PD inhibition, is responsible for the
downregulation of *Srf* expression, we measured *Srf* in SMCs cultured in Nx and Hx, and treated with G6PD
inhibitor and MEG3 siRNA. G6PD inhibition decreased *Srf* expression level in Nx- and Hx-SMCs (Fig. 5B).
Furthermore, MEG3 siRNA increased *Srf* expression in Nx-SMCs and G6PD inhibitor was not able to suppress
Srf expression in Nx- and Hx-SMCs treated with MRG siRNA (Fig. 5B).

Discussion

We sought to identify genes that were altered in the lungs of hypoxic mice through unbiased RNA-seq
analysis. In the lungs of hypoxic mice, >300 genes were upregulated and >1,500 genes were downregulated as
compared to those in normoxic mice. Among the upregulated genes, *Bnc2* and *Srf*, which encode transcription
factors, *Cbx8* and *Kdm1a*, which encode epigenetic modifiers, and *Pum2*, which encodes RNA-binding protein
that repress translational of cell differentiation proteins, appeared to top the list. Notably, most of the down-
regulated genes were related to nerve function, anticancer, and anticoagulation pathways. *Srf* is of particular
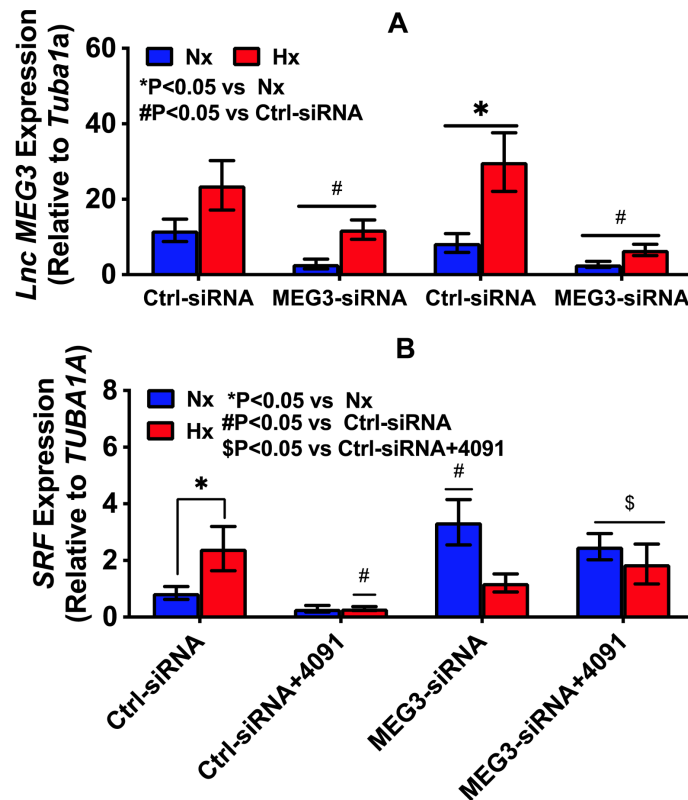
Fig. 5. G6PD inhibitor and MEG-3 siRNA regulates *Srf* expression in human pulmonary arterial SMCs. A) MEG3 expression level is decreased by MEG3-siRNA (50 nmol/l) in human pulmonary arterial SMCs exposed to normoxia (Nx; 21% O_2) and hypoxia (Hx; 3% O_2). Administration of 4091 (1 µmol/l) to human pulmonary arterial SMCs cultured under Nx or Hx upregulated MEG3 expression and this was blocked by MEG3-siRNA (50 nmol/l). There were no differences in expression of MEG3 between the application of control-siRNA with and without 4091. B) *Srf* expression in human SMCs exposed to Nx or Hx and treated with 4091 (1 µmol/l) and control (Ctrl)- or MEG3-siRNA (50 nmol/l). N=5–6. Statistical analysis was performed using the one-way ANOVA. Sidak's test was used to compare multiple groups after ANOVA analysis.

interest in the context of arterial wall remodeling because it encodes a transcription factor that selectively induces expression of all hallmark CArG-dependent, SMC-restricted genes through its interaction with MYOCD (35–37). Therefore, we speculated that increased *Srf* expression level would lead to augmented expression of SMC-restricted genes in the lungs of hypoxic mice. In contrast, Hx downregulated expression of *Myocd* and SRF-MYOCD-driven expression of *Cnn1* and *Myh11*, which encode MYH11 and CNN1, two proteins involved in maintaining vascular tone and contractility (40). These results are consistent with previous studies reporting suppressed MYH11 and CNN1 expression in SMCs obtained from hypoxic rats and sheep (1, 8), and in the arteries of PH patients (9). Moreover, G6PD inhibition upregulates *Myocd* in SMCs from rat aorta and PA (29). In our study, we found that G6PD inhibition decreased *Srf* expression level and increased *Myocd* expression level in the lungs of hypoxic mice. Additionally, G6PD inhibition or knockdown increased the expression level of SRF-MYOCD-driven *Cnn1* and *Myh11*. These results suggest that Hx, respectively, activates and suppresses the transcription of *Srf* and SRF-MYOCD-driven genes, and G6PD inhibition can restore their expression to normal levels.

Various signaling pathways and factors modulate the expression of SMC-restricted genes. When the MYOCD levels are low, transcription factors like KLF4 and KLF5 competitively bind to SRF, enabling transi-

tion of SMCs from a differentiated to a dedifferentiated (hyperproliferative and synthetic) phenotype (41). Consistent with those results, KLF4 and E2F1, which promote SMC proliferation (41, 42), were the most enriched transcription factors on genes upregulated by Hx. Conversely, G6PD inhibition decreased KLF4 enriched genes and *Srf* expression in SMCs.

Although the loss of MYOCD clearly plays a key role in the Hx-induced phenotypic transition of SMCs, our understanding of the mechanisms regulating *Myocd* transcription is incomplete. Post-transcriptionally, MYOCD expression is finely regulated by microRNAs (43). DNA methylation studies of the lungs of hypoxic mice revealed that Hx-induced hypermethylation of the functional regions of *Myocd* and several other SMC differentiation marker genes and suppressed their expression. Intriguingly, G6PD inhibition led to hypomethylation of CpG regions of *Myocd* and other SMC differentiation marker genes and increased methylation of *Msx2*, which encodes MSX2 (a repressor of *Myocd* activity (44)), and *Klf15*, which encodes KLF15 (a regulator of SMC proinflammatory activation (45) and repressor of *Myocd* activity (46)), in the lungs of hypoxic mice. Recent studies, including ours, suggest that downregulation of TET2 expression contributes to the pathogenesis of Hx-induced PH in mice and idiopathic PH in humans (27, 47). Previously, we showed that G6PD inhibition upregulates *Tet2* expression, and that TET2 is critical to the reduction in PA remodeling and PH associated with G6PD inhibition (27). Downregulation of TET2 increases DNA methylation and blocks promoter binding of transcription factors and transcription enhancers (48). This also increases binding of transcription repressors to the promoter. Both of these processes reduce transcription of the affected genes. Therefore, we suggest that G6PD-dependent TET2 downregulation may have potentially increased hypermethylation of genes and decreased pulmonary expression level of *Myocd* and SRF-MYOCD-driven genes in the lungs of hypoxic mice and in hypoxic SMCs. Additionally, G6PD inhibition hypomethylated *Kcnmb1* promoter and restored the expression of *Kcnmb1* and other genes encoding channel proteins in the lungs of hypoxic mice. Based on these findings, we propose that increased SRF-MYOCD-driven *Kcnmb1* expression level associated with G6PD inhibition restores the SMC phenotype and Ca^{2+} homeostasis and contributes to relax SMCs. Although, Hx-induced and G6PD-dependent DNA methylation appears to be functionally important for downregulating the expression of SMC differentiation marker genes in the hypoxic SMCs and lungs/PAs of hypoxic mice, expression of *Srf* gene was not controlled by DNA methylation.

We found that silencing MEG3 expression increased *Srf* transcription in hypoxic SMCs. Since G6PD inhibition decreased *Srf* expression in the lungs of mice and SMCs exposed to Hx, we speculated that MEG3, increased by G6PD inhibition, potentially mediated downregulation of *Srf* expression. Further, G6PD inhibitor in the presence of MEG siRNA did not decrease *Srf* expression. LncRNAs are biologically active molecules involved in various cellular processes, including genomic imprinting, chromatin remodeling, cell-cycle control, cell differentiation, and cell migration (49–51). They have emerged as critical modifiers of gene transcription that act by interacting with DNA, PRC-2 and JARID, and miRNA (52). To this regard, MEG3 acts as an epigenetic modifier that, along with PRC-2 and JARID2, mediates addition of repressive H3K9me and H3K27me marks to genes (26, 53). Although MEG3 expression in the lungs of hypoxic mice was not different from that of normoxic mice, G6PD inhibition hypomethylated MEG3 gene in the promoter flank region and increased MEG3 expression level in the lungs of mice and in SMCs exposed to Hx. These findings reveal previously unknown endogenous controller of MEG transcription in the hypoxic SMC. MEG3 prevents SMC proliferation and are consistent with a previous study that suggested loss of MEG3 promotes pulmonary arterial SMC proliferation (21). This represents a MEG3-dependent pathway through which G6PD inhibition prevented hypoxia-induced *Srf* gene, which encodes a transcription factor, and SMC dedifferentiation genes. Dedifferentiated SMCs secrete extracellular matrix proteins, inflammatory cytokines and chemokines, and growth factors,

which may contribute to a remodeled vasculature (5, 54).

In conclusion, the main results of this study collectively demonstrate that: 1) G6PD contributes to increase hypoxia-elicited expression level of *Srf* and decreased expression level of SMC genes (*Myocd*, *Cnn1*, and *Myh11*); 2) G6PD inhibition enhanced MEG3 expression and suppressed *Srf* expression in a MEG3-dependent manner in hypoxic SMCs; and 3) G6PD inhibition mediated DNA hypomethylation increased expression of SRF-MYOCD-driven genes in hypoxic lungs/PAs. Thus, G6PD, a key redox hub, and MEG3 appears to be a potentially useful target for restoring pulmonary arterial expression of SMC protein-encoding genes and ion channels to reduce hypoxia-induced SMC dedifferentiation.

Funding

Conflict of Interest

No conflict of interest to disclose.

References

1. Chettimada S, Gupte R, Rawat D, Gebb SA, McMurtry IF, Gupte SA. Hypoxia-induced glucose-6-phosphate dehydrogenase overexpression and -activation in pulmonary artery smooth muscle cells: implication in pulmonary hypertension. Am J Physiol Lung Cell Mol Physiol. 2015; 308(3): L287–300. [Medline] [CrossRef]

2. Circu ML, Aw TY. Reactive oxygen species, cellular redox systems, and apoptosis. Free Radic Biol Med. 2010; 48(6): 749–62. [Medline] [CrossRef]

3. Frid MG, Dempsey EC, Durmowicz AG, Stenmark KR. Smooth muscle cell heterogeneity in pulmonary and systemic vessels. Importance in vascular disease. Arterioscler Thromb Vasc Biol. 1997; 17(7): 1203–9. [Medline] [CrossRef]

4. Frid MG, Aldashev AA, Dempsey EC, Stenmark KR. Smooth muscle cells isolated from discrete compartments of the mature vascular media exhibit unique phenotypes and distinct growth capabilities. Circ Res. 1997; 81(6): 940–52. [Medline] [CrossRef]

5. Morrell NW, Adnot S, Archer SL, Dupuis J, Lloyd Jones P, MacLean MR, et al. Cellular and molecular basis of pulmonary arterial hypertension. J Am Coll Cardiol. 2009; 54(1 Suppl): S20–31. [Medline] [CrossRef]

6. Farber HW, Loscalzo J. Pulmonary arterial hypertension. N Engl J Med. 2004; 351(16): 1655–65. [Medline] [CrossRef]

7. Frismantiene A, Philippova M, Erne P, Resink TJ. Smooth muscle cell-driven vascular diseases and molecular mechanisms of VSMC plasticity. Cell Signal. 2018; 52: 48–64. [Medline] [CrossRef]

8. Zhou W, Negash S, Liu J, Raj JU. Modulation of pulmonary vascular smooth muscle cell phenotype in hypoxia: role of cGMP-dependent protein kinase and myocardin. Am J Physiol Lung Cell Mol Physiol. 2009; 296(5): L780–9. [Medline] [CrossRef]

9. Sahoo S, Meijles DN, Al Ghouleh I, Tandon M, Cifuentes-Pagano E, Sembrat J, et al. MEF2C-MYOCD and Leiomodin1 suppression by miRNA-214 promotes smooth muscle cell phenotype switching in pulmonary arterial hypertension. PLoS One. 2016; 11(5): e0153780. [Medline] [CrossRef]

10. Sheikh AQ, Misra A, Rosas IO, Adams RH, Greif DM. Smooth muscle cell progenitors are primed to muscularize in pulmonary hypertension. Sci Transl Med. 2015; 7(308): 308ra159. [Medline] [CrossRef]

11. Boucherat O, Vitry G, Trinh I, Paulin R, Provencher S, Bonnet S. The cancer theory of pulmonary arterial hypertension. Pulm Circ. 2017; 7(2): 285–99. [Medline] [CrossRef]

12. D'Alessandro A, El Kasmi KC, Plecitá-Hlavatá L, Ježek P, Li M, Zhang H, et al. Hallmarks of pulmonary hypertension: mesenchymal and inflammatory cell metabolic reprogramming. Antioxid Redox Signal. 2018; 28(3): 230–50. [Medline] [CrossRef]

13. Li M, Riddle S, Zhang H, D'Alessandro A, Flockton A, Serkova NJ, et al. Metabolic reprogramming regulates the proliferative and inflammatory phenotype of adventitial fibroblasts in pulmonary hypertension through the transcriptional corepressor C-terminal binding protein-1. Circulation. 2016; 134(15): 1105–21. [Medline] [CrossRef]

14. Yao C, Yu J, Taylor L, Polgar P, McComb ME, Costello CE. Protein expression by human pulmonary artery smooth muscle cells containing a *BMPR2* mutation and the action of ET-1 as determined by proteomic mass spectrometry. Int J Mass Spectrom. 2015; 378: 347–59. [Medline] [CrossRef]

15. Boehme J, Sun X, Tormos KV, Gong W, Kellner M, Datar SA, et al. Pulmonary artery smooth muscle cell hyperproliferation and metabolic shift triggered by pulmonary overcirculation. Am J Physiol Heart Circ Physiol. 2016; 311(4): H944–57. [Medline] [CrossRef]

16. Sun X, Kumar S, Sharma S, Aggarwal S, Lu Q, Gross C, et al. Endothelin-1 induces a glycolytic switch in pulmonary arterial endothelial cells via the mitochondrial translocation of endothelial nitric oxide synthase. Am J Respir Cell Mol Biol. 2014; 50(6): 1084–95. [Medline] [CrossRef]

17. Chettimada S, Joshi SR, Alzoubi A, Gebb SA, McMurtry IF, Gupte R, et al. Glucose-6-phosphate dehydrogenase plays a critical role in hypoxia-induced CD133+ progenitor cells self-renewal and stimulates their accumulation in the lungs of pulmonary hypertensive rats. Am J Physiol Lung Cell Mol Physiol. 2014; 307(7): L545–56. [Medline] [CrossRef]

18. Mercer TR, Dinger ME, Mattick JS. Long non-coding RNAs: insights into functions. Nat Rev Genet. 2009; 10(3): 155–9. [Medline] [CrossRef]

19. Chen YG, Satpathy AT, Chang HY. Gene regulation in the immune system by long noncoding RNAs. Nat Immunol. 2017; 18(9): 962–72. [Medline] [CrossRef]

20. Haemmig S, Simion V, Yang D, Deng Y, Feinberg MW. Long noncoding RNAs in cardiovascular disease, diagnosis, and therapy. Curr Opin Cardiol. 2017; 32(6): 776–83. [Medline] [CrossRef]

21. Sun Z, Nie X, Sun S, Dong S, Yuan C, Li Y, et al. Long non-coding RNA MEG3 downregulation triggers human pulmonary artery smooth muscle cell proliferation and migration via the p53 signaling pathway. Cell Physiol Biochem. 2017; 42(6): 2569–81. [Medline] [CrossRef]

22. Ahmed ASI, Dong K, Liu J, Wen T, Yu L, Xu F, et al. Long noncoding RNA *NEAT1* (nuclear paraspeckle assembly transcript 1) is critical for phenotypic switching of vascular smooth muscle cells. Proc Natl Acad Sci USA. 2018; 115(37): E8660–7. [Medline] [CrossRef]

23. Bell RD, Long X, Lin M, Bergmann JH, Nanda V, Cowan SL, et al. Identification and initial functional characterization of a human vascular cell-enriched long noncoding RNA. Arterioscler Thromb Vasc Biol. 2014; 34(6): 1249–59. [Medline] [CrossRef]

24. Boon RA, Hofmann P, Michalik KM, Lozano-Vidal N, Berghäuser D, Fischer A, et al. Long noncoding RNA Meg3 controls endothelial cell aging and function: implications for regenerative angiogenesis. J Am Coll Cardiol. 2016; 68(23): 2589–91. [Medline] [CrossRef]

25. Zhao J, Zhang W, Lin M, Wu W, Jiang P, Tou E, et al. MYOSLID is a novel serum response factor-dependent long noncoding RNA that amplifies the vascular smooth muscle differentiation program. Arterioscler Thromb Vasc Biol. 2016; 36(10): 2088–99. [Medline] [CrossRef]

26. Kaneko S, Bonasio R, Saldaña-Meyer R, Yoshida T, Son J, Nishino K, et al. Interactions between JARID2 and noncoding RNAs regulate PRC2 recruitment to chromatin. Mol Cell. 2014; 53(2): 290–300.

[Medline] [CrossRef]

27. Joshi SR, Kitagawa A, Jacob C, Hashimoto R, Dhagia V, Ramesh A, et al. Hypoxic activation of glucose-6-phosphate dehydrogenase controls the expression of genes involved in the pathogenesis of pulmonary hypertension through the regulation of DNA methylation. Am J Physiol Lung Cell Mol Physiol. 2020; 318(4): L773–86. [Medline] [CrossRef]

28. Reisz JA, Tzounakas VL, Nemkov T, Voulgaridou AI, Papassideri IS, Kriebardis AG, et al. Metabolic linkage and correlations to storage capacity in erythrocytes from glucose 6-phosphate dehydrogenase-deficient donors. Front Med (Lausanne). 2018; 4: 248. [Medline] [CrossRef]

29. Chettimada S, Joshi SR, Dhagia V, Aiezza A 2nd, Lincoln TM, Gupte R, et al. Vascular smooth muscle cell contractile protein expression is increased through protein kinase G-dependent and -independent pathways by glucose-6-phosphate dehydrogenase inhibition and deficiency. Am J Physiol Heart Circ Physiol. 2016; 311(4): H904–12. [Medline] [CrossRef]

30. Rajasekaran NS, Connell P, Christians ES, Yan LJ, Taylor RP, Orosz A, et al. Human alpha B-crystallin mutation causes oxido-reductive stress and protein aggregation cardiomyopathy in mice. Cell. 2007; 130(3): 427–39. [Medline] [CrossRef]

31. Ali ZA, de Jesus Perez V, Yuan K, Orcholski M, Pan S, Qi W, et al. Oxido-reductive regulation of vascular remodeling by receptor tyrosine kinase ROS1. J Clin Invest. 2014; 124(12): 5159–74. [Medline] [CrossRef]

32. Hamilton NM, Dawson M, Fairweather EE, Hamilton NS, Hitchin JR, James DI, et al. Novel steroid inhibitors of glucose 6-phosphate dehydrogenase. J Med Chem. 2012; 55(9): 4431–45. [Medline] [CrossRef]

33. Kitagawa A, Jacob C, Jordan A, Waddell I, McMurtry IF, Gupte SA. Inhibition of glucose-6-phosphate dehydrogenase activity attenuates right ventricle pressure and hypertrophy elicited by VEGFR inhibitor + hypoxia. J Pharmacol Exp Ther. 2021; 377(2): 284–92. [Medline] [CrossRef]

34. Kwon AT, Arenillas DJ, Worsley Hunt R, Wasserman WW. oPOSSUM-3: advanced analysis of regulatory motif over-representation across genes or ChIP-Seq datasets. G3 (Bethesda). 2012; 2(9): 987–1002. [Medline] [CrossRef]

35. Wang D, Chang PS, Wang Z, Sutherland L, Richardson JA, Small E, et al. Activation of cardiac gene expression by myocardin, a transcriptional cofactor for serum response factor. Cell. 2001; 105(7): 851–62. [Medline] [CrossRef]

36. Chen J, Kitchen CM, Streb JW, Miano JM. Myocardin: a component of a molecular switch for smooth muscle differentiation. J Mol Cell Cardiol. 2002; 34(10): 1345–56. [Medline] [CrossRef]

37. Yoshida T, Sinha S, Dandré F, Wamhoff BR, Hoofnagle MH, Kremer BE, et al. Myocardin is a key regulator of CArG-dependent transcription of multiple smooth muscle marker genes. Circ Res. 2003; 92(8): 856–64. [Medline] [CrossRef]

38. Kaplan-Albuquerque N, Van Putten V, Weiser-Evans MC, Nemenoff RA. Depletion of serum response factor by RNA interference mimics the mitogenic effects of platelet derived growth factor-BB in vascular smooth muscle cells. Circ Res. 2005; 97(5): 427–33. [Medline] [CrossRef]

39. Cheng X, Wang Y, Du L. Epigenetic modulation in the initiation and progression of pulmonary hypertension. Hypertension. 2019; 74(4): 733–9. [Medline] [CrossRef]

40. Kim HR, Appel S, Vetterkind S, Gangopadhyay SS, Morgan KG. Smooth muscle signalling pathways in health and disease. J Cell Mol Med. 2008; 12(6A): 2165–80. [Medline] [CrossRef]

41. Liu Y, Sinha S, McDonald OG, Shang Y, Hoofnagle MH, Owens GK. Kruppel-like factor 4 abrogates myocardin-induced activation of smooth muscle gene expression. J Biol Chem. 2005; 280(10): 9719–27. [Medline] [CrossRef]

42. Shelat HS, Liu TJ, Hickman-Bick DL, Barnhart MK, Vida T, Dillard PM, et al. Growth suppression of human coronary vascular smooth muscle cells by gene transfer of the transcription factor E2F-1. Circu-

lation. 2001; 103(3): 407–14. [Medline] [CrossRef]

43. Cordes KR, Sheehy NT, White MP, Berry EC, Morton SU, Muth AN, et al. miR-145 and miR-143 regulate smooth muscle cell fate and plasticity. Nature. 2009; 460(7256): 705–10. [Medline] [CrossRef]

44. Hayashi K, Nakamura S, Nishida W, Sobue K. Bone morphogenetic protein-induced MSX1 and MSX2 inhibit myocardin-dependent smooth muscle gene transcription. Mol Cell Biol. 2006; 26(24): 9456–70. [Medline] [CrossRef]

45. Lu Y, Zhang L, Liao X, Sangwung P, Prosdocimo DA, Zhou G, et al. Kruppel-like factor 15 is critical for vascular inflammation. J Clin Invest. 2013; 123(10): 4232–41. [Medline] [CrossRef]

46. Leenders JJ, Wijnen WJ, Hiller M, van der Made I, Lentink V, van Leeuwen REW, et al. Regulation of cardiac gene expression by KLF15, a repressor of myocardin activity. J Biol Chem. 2010; 285(35): 27449–56. [Medline] [CrossRef]

47. Potus F, Pauciulo MW, Cook EK, Zhu N, Hsieh A, Welch CL, et al. Novel mutations and decreased expression of the epigenetic regulator *TET2* in pulmonary arterial hypertension. Circulation. 2020; 141(24): 1986–2000. [Medline] [CrossRef]

48. Solary E, Bernard OA, Tefferi A, Fuks F, Vainchenker W. The Ten-Eleven Translocation-2 (TET2) gene in hematopoiesis and hematopoietic diseases. Leukemia. 2014; 28(3): 485–96. [Medline] [CrossRef]

49. Rinn JL, Chang HY. Genome regulation by long noncoding RNAs. Annu Rev Biochem. 2012; 81: 145–66. [Medline] [CrossRef]

50. Sun M, Gadad SS, Kim DS, Kraus WL. Discovery, annotation, and functional analysis of long noncoding RNAs controlling cell-cycle gene expression and proliferation in breast cancer cells. Mol Cell. 2015; 59(4): 698–711. [Medline] [CrossRef]

51. Jaé N, Heumüller AW, Fouani Y, Dimmeler S. Long non-coding RNAs in vascular biology and disease. Vascul Pharmacol. 2019; 114: 13–22. [Medline] [CrossRef]

52. Ponting CP, Oliver PL, Reik W. Evolution and functions of long noncoding RNAs. Cell. 2009; 136(4): 629–41. [Medline] [CrossRef]

53. Gardner KE, Allis CD, Strahl BD. Operating on chromatin, a colorful language where context matters. J Mol Biol. 2011; 409(1): 36–46. [Medline] [CrossRef]

54. Stenmark KR, Fagan KA, Frid MG. Hypoxia-induced pulmonary vascular remodeling: cellular and molecular mechanisms. Circ Res. 2006; 99(7): 675–91. [Medline] [CrossRef]